Original Article
Running Title: Tumor Microenvironment's Influence on SLC4A7 (NBCn1) and Caspase-3 Genes in Breast Cancer, along with In Silico Characteristics of NBCn1
Received: July 12, 2023; Accepted: February 05, 2024

A Mimicry of the Tumor Microenvironment's Impact on SLC4A7 (NBCn1) and Caspase-3 Gene Expression in Breast Cancer, along with in Silico Traits of NBCn1

Amin Mehra[*], Pharm.D, Reza Mehrkar[**], BSc, Amir Fakhri[***], MSc, Pedram Jabbari Fard[****], BSc, Mohammad Reza Asgharzadeh[***♦], PhD, Mohammad Hossein Ghaffari Agdam[****], MSc, Rasoul Sharifi[*****♦] PhD

[*]*Faculty of Pharmacy, Tabriz University of Medical Sciences, Tabriz, Iran*
[**]*Department of Medical Laboratory Sciences, Faculty of Paramedicine, Tabriz University of Medical Sciences, Tabriz, Iran*
[***]*Department of Biology, Urmia Branch, Islamic Azad University, Urmia, Iran*
[****]*Department of Microbiology, Faculty of Basic Science, Science and Research Branch, Islamic Azad University, Tehran, Iran*
[*****]*Department of Biology, Ahar Branch, Islamic Azad University, Ahar, Iran*

♦Corresponding Author
Rasoul Sharifi, PhD
Department of Biology, Ahar Branch,
Islamic Azad University, Ahar, Iran
Email: rasoulsharifi.sci@gmail.com

Abstract

Background: This study investigates the relative expression of the Na^+, HCO_3^- cotransport gene NBCn1, and caspase-3 within the tumor microenvironment of human breast cancer, considering the in vivo microenvironment.

Method: In this experimental study, breast cancer MDA-MB-231 cells were cultured under normoxia/hypoxia conditions for 24, 48, and 72 hours with varying glucose concentrations (5.5, 11, and 25 mM). The mRNA expression of NBCn1 and caspase-3 was evaluated using real-time polymerase chain reaction. The stability and binding pocket of NBCn1 were assessed using DispHred and the Computed Atlas of Surface Topography of proteins (CASTp) servers, respectively. The location prediction of the protein was determined using the Transmembrane Helices; Hidden Markov Model (TMHMM) server.

Results: Normoxia led to an increase in NBCn1 expression during all three time periods, displaying heterogeneity. The expression was particularly elevated at glucose concentrations of 25 and 5.5 mM. In hypoxic conditions, gene expression was reduced; however, an increase in glucose concentration enhanced SLC4A7 expression. Specifically, a glucose concentration of 25 mM led to decreased caspase-3 expression under hypoxic conditions. In silico studies revealed that SLC4A7 becomes disordered when the pH falls below 7, with most amino acids in the binding pocket being nonpolar.

Conclusion: The heightened risk of breast cancer metastasis may be linked to the upregulation of SLC4A7 and downregulation of caspase-3 expression, underscoring their fundamental roles in

cancer treatment and prevention. SLC4A7 is a transmembrane protein, and its folding is pH-dependent.
Keywords: Tumor microenvironment, SLC4A7, Caspase-3, Breast neoplasms, In silico

Introduction

Breast cancer is a highly occurring cancer, and it is the primary cause of cancer deaths among women all over the globe.[1] Breast cancer has been considered a very heterogeneous group of diseases differing in molecular and genetic traits, pathogenesis characteristics, clinical period, and response to treatment.[2] Efforts have been directed towards developing and optimizing in vitro systems closely mimicking the in vivo environment to understand intercellular communication while permitting a simplified approach. The tumor microenvironment (TME) is intricate, including carcinoma cells co-existing and evolving with host stroma.[3,4] This stromal part comprises fibroblasts, myofibroblasts, endothelial cells, various immune parts, and an extracellular matrix. The carcinoma-associated fibroblasts (CAFs), contrary to non-activated and normal fibroblasts, contribute to tumor initiation, progression, angiogenesis, invasion, metastasis, and recurrence in various carcinomas, including breast, prostate, lung, pancreas, skin, colon, esophagus, and ovary.[5] The disruption of pH in the region of cancer cells is a critical step in the development of the tumor to the metastasis stage. Extracellular acidosis is typically found in solid cancers. Pyruvate is converted to lactic acid by lactate dehydrogenase under anaerobic conditions. Furthermore, the Warburg effect, in which pyruvic acid is converted to lactic acid under aerobic conditions, occurs also in cancer cells.[6,7] Exceedingly production of lactic acid causes its extracellular release and extracellular acidosis.[8] The low pH of the tumorous region is related to increased metastasis and proliferation by inducing an abnormal phenotype and inhibiting immune cell activity.[9]

Membrane acid-base transport is an essential pathway for disposing of cellular acid and can be mediated by different membrane proteins. Based on studies in the human MCF-7 breast cancer cell line.[10] Na^+ dependent HCO_3^- transport has been suggested as a fundamental mechanism for net acid extrusion in cancer cell lines.[11]

The sodium bicarbonate co-transporter NBCn1/Slc4a7 is involved in the uptake of Na^+ and HCO_3^- into cells in an electroneutral manner.[12] The HCO_3^- transport using NBCn1 resulted in intracellular pH (pHi) adjusting in various cell types and facilitated the release of transepithelial HCO_3^- and absorption across epithelial cells.[12]

This acidity distribution favors cancer growth since a high pHi is vital for cancer cell development and survival; on the contrary, a low pHo is crucial for migration and invasiveness of the cancer cells. Moreover, the microenvironment in some cancers has been found to change the protein expression and cell signaling in the tumor cells, supporting their invasiveness and suppressing apoptosis and immune response.[13] Ligands, binding partners, or solvent traits, such as ion concentration or pH, are essential to folding some proteins.[14] Therefore, it is beneficial to follow those effects in computational approaches. Undoubtedly, it is clear that the C–H (Charge–hydropathy) relationship of a given protein is changeable since sequence-related factors can affect both protein net charge and hydrophobicity.[15]

Caspase-3, a leading protein, is located at crucial parts of signal pathways, and it takes part in various activities such as regulating the cell cycle and the invasion and metastatic,

the immune cell activity and cytokine production, two primary components of the TME.[16] Caspase-3 expression has often been dysregulated by breast cancer, leading to an imbalance between its apoptotic and non-apoptotic functions within the tumor and the surrounding milieu.

Thus, this study aimed to investigate the impacts of different concentrations of glucose and hypoxia on SLC4A7 (NBCn1) and caspase-3 gene expression in MDA-MB-231 cell lines and to evaluate some computational stability of NBCn1 in silico situations.

Material and Methods

Cell culture

In this experimental study, the Pasteur Institute of Iran provided MDA-MB-231 cells cultured in Roswell Park Memorial Institute (RPMI) 1640 medium (Gibco, England). The culture medium contained 10% fetal bovine serum (Gibco, South America) and 1% penicillin/streptomycin (Bioidea, Iran). The cells were incubated in a humidified cell culture incubator at 37°C with 5% CO_2. Generating these cancer cells closely mimics the process in the human body.

To investigate their interaction with the physiological environment, the cultured cells were exposed to different glucose concentrations (5.5, 11, and 25 mM) and varying oxygen levels (hypoxia and normoxia). Hypoxic conditions were induced using Cobalt(II) Chloride ($CoCl_2$) (Sigma Aldrich, Germany) at a concentration of 150 µM in the cell culture.

Since angiogenesis in tumor tissue differs from normal tissue, and the vascular pores within tumor tissue vary from normal tissue, oxygen, and glucose levels within the tumor can be heterogeneous. In specific regions of the tumor tissue, oxygen and glucose levels have remained at average physiological concentrations. Therefore, a glucose concentration of 11 mM and an oxygen level of 21% was maintained in the cell culture for these regions. Conversely, in regions where the exchange rates were elevated due to increased angiogenesis and larger pores, 25 mM of glucose was used; for regions with low angiogenesis, 5.5 mM glucose was employed. Hypoxic conditions were simulated by reducing the oxygen concentration to 1% in the cell culture.

This experimental approach allows us to study how varying glucose and oxygen concentrations influence the behavior of MDA-MB-231 cells, shedding light on their responses in different microenvironments.

Extraction of total RNA and complementary synthesis of complementary DNA (cDNA)

The BioFACT^{TM} Total RNA Prep Kit (Biofact, Yuseong-Gu, Daejeon, South Korea) was utilized to extract RNA from the cells. Meticulously adhering to the protocol provided with the kit ensured the successful extraction of RNA.

The purity of the isolated RNA was quantified using a NanoDrop device (Nano Mabna, Iran), which measures the optical density.

Subsequently, the RNA extracted from the MDA-MB-231 cell line was used for cDNA synthesis. This process was carried out using the Biofact Synthesis of cDNA Kit protocol. The reaction mixture comprised 10 ng of total RNA, 1 µL of Random Hexamer Primers, 10 µL of 2X RT pre-mix, and approximately 8 µL of RNase-free water (Biofact, Yuseong-Gu, Daejeon, South Korea). The synthesis was facilitated by a precise thermal cycling program, which included an initial step at room temperature for 5 minutes, a 30-minute incubation at 50°C, and a final denaturation step at 95°C for 5 minutes.

Primer design and real-time polymerase chain reaction (PCR)

Primers were meticulously designed for the NBCn1 (SLC4A7), caspase-3, and Actin Beta (ACTB) genes using resources from the

National Center for Biotechnology Information (NCBI) and employing the Oligo analysis software, version 7. The real-time PCR assays were conducted in a 25 µL reaction volume. Each well of the assay comprised the following components: 1 µL of cDNA, 10 pmol/µL of forward primer, 10 pmol/µL of reverse primer, 12.5 µL of Master Mix SYBR Green (Biofact, Yuseong-Gu, Daejeon, South Korea), and 9.5 µL of RNase/DNase-free water.

The thermal cycling conditions were meticulously programmed as follows: an initial denaturation at 95°C for 10 minutes, followed by 40 cycles of denaturation at 95°C for 20 seconds, annealing at 61-63°C (temperature varied depending on the specific gene) for 20 seconds, and extension at 72°C for 30 seconds, with a final extension at 72°C for 5 minutes. Roche, Germany, provided the thermocycler used for the process. Details of the primers used are listed in table 1.

Bioinformatics studies

Prediction of transmembrane helices in proteins using TMHMM server v. 2.0

TMHMM is a method for predicting membrane protein topology based on a Markov model. This server predicts transmembrane helices and determines soluble and membrane proteins with maximum accuracy. This server is dependent on FASTA format sequences up to 4000 protein sequences.[17]

DispHred, protein disorder predictor over pH for proteins

The DispHred web server is based on the Django 3.0 framework working with Python 3.7, and the matplotlib library creates figures. The server is accessible and available for academic aims.[18]

This server uses the pH-dependent lipophilicity score of Zamora and coworkers. Their solvation calculation measures the hydrophobicity of a given residue at the desired pH.[19]

The results were averaged to calculate the mean hydrophobicity of the sequence at the given pH. Protein NCPR (Net charge per residue) is calculated using the Henderson–Hasselbalch equation to determine the partial charge of each ionizable residue at the given pH. Then, total NCPR is measured as the sum of all partial charges. The residues that are in the given window and their length are essential for calculating NCPR and then DispH Score.[20]

Evaluation of protein stability and aliphatic indices

Protein sequence analysis can be conducted using various computational tools, among which the ProtParam tool on the ExPASy Proteomics Server is notably utilized. A critical metric derived from this analysis is the instability index (II), which indicates protein stability. According to the ProtParam guidelines, a protein is stable if the instability index is below 40. Conversely, a value above this threshold suggests the protein is inherently unstable, implying a shorter half-life in vivo. The analysis conducted via the ProtParam server revealed an instability index of 49.92 for the protein under study, categorizing it as unstable.

Identification of binding site using CASTp 3.0

Geometric and topological characteristics of protein structures, involving surface pockets, inner cavities, and channels, are of radical importance for proteins to perform their functions. Computed Atlas of Surface Topography of proteins (CASTp) is a web server that supplies online services for locating, determining, and measuring topological properties of proteins.[21]

Results

Analysis of cell morphology in MDA-MB-231 cells under normoxia and hypoxia conditions

Cell morphology remodels in MDAMB-231 cells

Figure 1 illustrates the morphological alterations in MDA-MB-231 cells subjected to varying oxygen tensions (hypoxia at 1% O_2 and normoxia at 20% O_2) and glucose concentrations (5.5, 11, and 25 mM) over time intervals of 24, 48, and 72 hours.[22] The observations highlighted a pronounced proliferation and robust growth of MDA-MB-231 cells in normoxic conditions compared to those in hypoxic environments. Under hypoxic stress, however, the cells exhibited notable resilience and managed to maintain their morphological characteristics, especially after 72 hours, indicating an adaptation and maximal compatibility with the hypoxic conditions.

Temporal dynamics of SLC4A7 (NBCn1) gene expression in MDA-MB-231 cells

The expression levels of the SLC4A7 gene in MDA-MB-231 cells across various time points were quantitatively assessed using the real-time PCR technique. Total RNA was extracted, and the relative expression of the SLC4A7 gene was normalized against the B-Actin gene as a control. The analysis revealed that under normoxic conditions, there was a heterogeneous yet progressive increase in SLC4A7 gene expression at 24, 48, and 72 hours within the MDA-MB-231 cell line. This upward trend in gene expression was particularly notable at two specific glucose concentrations.

Conversely, in hypoxic conditions, SLC4A7 expression was generally subdued. Nevertheless, elevated glucose levels were observed to induce the expression of the SLC4A7 gene. Notably, after 72 hours, the expression levels of SLC4A7 converged, hinting at the cell line's adaptive response to hypoxia and its potential role in regulating acidic metabolite production (refer to Figures 2-4 for detailed expression profiles).

Temporal dynamics of caspase-3 gene expression in MDA-MB-231 cells

Similar to the previous analysis, the expression levels of the caspase-3 gene in MDA-MB-231 cells were assessed using the real-time PCR technique. The total RNA was extracted, and the expression of the caspase-3 gene was normalized against the B-Actin gene. The findings indicated a negative correlation between glucose concentration and caspase-3 expression in a hypoxic environment, with the influence being markedly pronounced at a concentration of 25 mM. Parallel observations were recorded under normoxic conditions, where an increase in glucose concentration corresponded to a decrease in caspase-3 expression. However, due to extensive cell death at the 72-hour mark, gene expression data could not be reliably presented for this time point (Figures 5 and 6).

In silico analysis results

1. ***Results from TMHMM server:*** According to the TMHMM server analysis, NBCn1 is identified as a transmembrane protein, with a length of 1093 amino acids and comprising 11 transmembrane helices (TMHs). The detailed structure and sequence are visualized in figure 7.
2. ***Results from DisPhred server:*** The DisPhred server evaluates protein disorder across pH values, providing results in JSON or ZIP formats, including DisPhred calculations and graphical representations. The accompanying table summarizes the DisPhred scores, hydrophobicity, and Net Charge Per Residue (NCPR) at specified pH levels. A graph highlights the average DisPhred score per pH, with scores above the red dashed line indicating predicted order. Regions of the protein

sequence are color-coded to represent folded (green), disordered (red), and conditionally disordered (blue) segments. Notably, proteins with an NCPR below 0.25 are associated with compact globular structures, whereas values above this threshold indicate expanded, well-solvated coils (Figure 8).

3. ***Results from CASTp 3.0 server:*** Analysis by the CASTp 3.0 server reveals the cooperative interaction of two chains in forming a cavity and binding pockets. Specifically, residues Lys102, Pro103, Tyr104, Val105, Thr107, Leu343, and Pro344 from Chain A, and residues Phe89, Lys102, Pro103, Tyr104, Val105, Ala106, Thr107, and Leu343 from Chain B contribute to the formation of these structural features (Figure 9).
4. ***ViewerLite software output:*** The ViewerLite software provides a detailed mapping of the amino acids constituting the binding pocket, clearly delineated in figure 10.

Discussion

This study's findings indicate that high glucose concentrations induce the upregulation of SLC4A7 and the downregulation of caspase-3 expression under hypoxic conditions. The in silico analysis revealed that the SLC4A7 protein is a transmembrane entity, predominantly composed of nonpolar amino acids contributing to its topology and the formation of the NBCn1 binding pocket. The DisPhred server's analysis suggested a significant retention of the protein's sequence integrity across unfavorable pH levels, highlighting its structural stability.

Hypoxia, a characteristic TMEfeature in most solid tumors, alters cellular metabolism. Without oxygen, cells shift their metabolic reliance from oxidative phosphorylation to alternative pathways, such as lactate dehydrogenase, leading to lactic acid production. [23]

The SLC4A7 protein (NBCn1), functioning as an electroneutral Na^+, HCO_3^- co-transporter, plays a pivotal role in regulating intracellular pH (pHi) by facilitating net acid extrusion in various cell lines,[24-28] including the human MCF-7 breast cancer cell line. Overexpression of NBCn1 is thought to contribute to maintaining a high pHi, fostering an environment conducive to cancer cell proliferation and survival, while simultaneously promoting a low extracellular pH (pHo), favorable for cancer cell migration and invasiveness.[29]

It has been reported that expression of the Na^+, HCO_3^- cotransporter NBCn1 is high in human primary breast carcinomas and metastases compared to normal breast tissue.[30]

Recently, have been demonstrated that breast cancerbicarbonate transporters, such as the electroneutral Na^+, HCO_3^- cotransporter (SLC4A7, NBCn1), are upregulated and play central roles in pH regulation.[31] Regarding tissue samples from women of European race, it has been shown that the plasma membrane expression of SLC4A7 is upregulated in human primary breast carcinomas and metastases in comparison with normal breast tissue.[32,33] Caspase-8 is a vital protein involved in cell cycle, apoptosis, invasive and metastatic behaviors, immune cell homeostasis, and cytokine production.[2] When caspase-8 is downregulated, Gynecological cancers such as breast and ovarian cancers seem to be more aggressive.[13,34] Dysregulated caspase expression causes an imbalance between the apoptotic and nonapoptotic functions in the primary tumor and the TME. Therefore, caspase-3 may be the link in the crosstalk between the tumor and the TME.[35-37]

The results of this study revealed that normoxia resulted in an increase in SLC4A7

expression as heterogenic in 24h, 48h, and 72h in the MDA-MB-231 cell line.

When the time went on, the gene expression increased in two concentrations. The gene expression was low in the hypoxia situation, yet high glucose concentration triggered the expression of SLC4A7. The level of SLC4A7 expression was closed together after 72 h, which may be an index of cell compatibility with a hypoxic atmosphere and production of acidic metabolites (Figures 2-4). Furthermore, the results revealed that an increase in glucose concentration led to a decrease in the expression of caspase-3 in hypoxic situations. The effect of 25mM was significant. The same results for caspase-3 expression with increased glucose concentration were found in normoxia. It is safe to conclude that an increase in glucose concentration leads to a decrease in agents involved in apoptosis (Figures 5 and 6).

In silico results showed that SLC4A7 is a transmembrane protein (Figure 7) and it is an unstable protein according to the instability index and ProtProm server (instability index = 49, index more than 40 is a criterion for protein instability, the results were not showed). The structures of proteins depend on their microenvironments. Binding agents to protein, organic molecules, or solutes can alter the protein's entirety, such as aggregation or order-disorder conformation. Many studies do not view the bioinformatics effect of pH on protein net charge and hydrophobicity. Pursuing the effect of pH on protein net charge, hydrophobicity might allow us to anticipate pH-dependent stability or conditional disorder of protein.

DispHred server showed that folding some sequences of SLC4A7 is strongly related to pH alteration while the huge sequence remains intact in undesirable pH amounts (Figure 8). All DispH amounts were positive, indices of the folded status of the protein. The hydrophobicity of protein was unchanged in the pH range between 6.9-7.4. One of the great forces triggering the folding of proteins is hydrophobicity. Generally, hydrophobic residues direct preferentially in the interior part of the protein, whereas polar residues are located at the exterior part of a folded protein.[38, 39] Polypeptides with large NCPR values can be viewed as "polyelectrolytes" and NCPR is close to zero and behaves as disordered globules directed by attractive interactions;[39] in this study, NCPR value for $pH_{6.9}$ was in the minimum range that is criteria of protein instability in this pH amount. The CASTp 3.0 server showed that nonpolar amino acids are predominant in topology and the formation of the binding pocket of NBCn1. A_{Lys102}, A_{Pro103}, A_{Tyr104}, $AVal_{105}$, A_{Thr107}, A_{Leu343} A_{Pro344} B_{Phe89}, B_{Lys102}, B_{Pro103}, B_{Tyr104}, B_{Val105}, B_{Ala106}, $BT_{hr107,}$ and B_{Leu343} are involved in making binding pocket (Figure 9).

Considering the number of carbon atoms in the substrate of NBCn1, the optimization of the substrate and study of protein-ligand interaction was impossible, which was the main obstacle for the authors of this study. Another issue is the impossibility of choosing 2.5mM glucose due to cellular death after 24 h; therefore, extracting real RNA was impossible.

Conclusion

Alterations in glucose concentration and hypoxic conditions were observed to modulate cancer cells' expression profiles significantly. Notably, the study documented the upregulation of SLC4A7 and the downregulation of caspase-3 under these conditions, linking these expression patterns to an increased risk of breast cancer metastasis. This underscores the pivotal roles of these genes in the mechanisms underlying cancer progression and highlights their potential as critical targets in cancer therapy and prevention strategies. Additionally, in silico analyses corroborated that the SLC4A7 protein is a transmembrane entity, with

nonpolar amino acids predominantly influencing its topology and the formation of the NBCn1 binding pocket, further enriching the understanding of its structural and functional dynamics.

Acknowledgments
The authors thank the laboratory experts for their invaluable technical support and contributions to this research. Their expertise and dedication were pivotal in facilitating the successful completion of this study.

Conflict of Interest
None declared.

References
1. Harbeck N, Gnant M. Breast cancer. *Lancet.* 2017;389(10074):1134-50. doi: 10.1016/S0140-6736(16)31891-8.
2. Payan N, Presles B, Brunotte F, Coutant C, Desmoulins I, Vrigneaud JM, et al. Biological correlates of tumor perfusion and its heterogeneity in newly diagnosed breast cancer using dynamic first-pass ^{18}F-FDG PET/CT. *Eur J Nucl Med Mol Imaging.* 2020;47(5):1103-15. doi: 10.1007/s00259-019-04422-4.
3. Xu X, Sun X, Ma L, Zhang H, Ji W, Xia X, et al. ^{18}F-FDG PET/CT radiomics signature and clinical parameters predict progression-free survival in breast cancer patients: A preliminary study. *Front Oncol.* 2023;13:1149791. doi: 10.3389/fonc.2023.1149791.
4. Incio J, Suboj P, Chin SM, Vardam-Kaur T, Liu H, Hato T, et al. Metformin reduces desmoplasia in pancreatic cancer by reprogramming stellate cells and tumor-associated macrophages. *PLoS One.* 2015;10(12):e0141392.
5. Zhang C, Fu L, Fu J, Hu L, Yang H, Rong TH, et al. Fibroblast growth factor receptor 2-positive fibroblasts provide a suitable microenvironment for tumor development and progression in esophageal carcinoma. *Clin Cancer Res.* 2009;15(12):4017-27
6. Liberti MV, Locasale JW. Correction to: 'The Warburg effect: How does it benefit cancer cells?': [Trends in Biochemical Sciences, 41 (2016) 211]. *Trends Biochem Sci.* 2016;41(3):287. doi: 10.1016/j.tibs.2016.01.004. Erratum for: *Trends Biochem Sci.* 2016;41(3):211-8.
7. Ivashkiv LB. The hypoxia-lactate axis tempers inflammation. *Nat Rev Immunol.* 2020;20(2):85-6. doi: 10.1038/s41577-019-0259-8.
8. Corbet C, Feron O. Tumour acidosis: from the passenger to the driver's seat. *Nat Rev Cancer.* 2017;17(10):577-93. doi: 10.1038/nrc.2017.77.
9. de la Cruz-López KG, Castro-Muñoz LJ, Reyes-Hernández DO, García-Carrancá A, Manzo-Merino J. Lactate in the regulation of tumor microenvironment and therapeutic approaches. *Front Oncol.* 2019;9:1143.
10. Lauritzen G, Stock CM, Lemaire J, Lund SF, Jensen MF, Damsgaard B, et al. The Na+/H+ exchanger NHE1, but not the Na+, HCO3(-) cotransporter NBCn1, regulates motility of MCF7 breast cancer cells expressing constitutively active ErbB2. *Cancer Lett.* 2012;317(2):172-83.
11. Hulikova A, Vaughan-Jones RD, Swietach P. Dual role of CO_2/HCO_3(-) buffer in the regulation of intracellular pH of three-dimensional tumor growths. *J Biol Chem.* 2011;286(16):13815-26. doi: 10.1074/jbc.M111.219899.
12. Boedtkjer E, Praetorius J, Matchkov VV, Stankevicius E, Mogensen S, Füchtbauer AC, et al. Disruption of Na^+,HCO_3^- cotransporter NBCn1 (slc4a7) inhibits NO-mediated vasorelaxation, smooth muscle Ca^{2+} sensitivity, and hypertension development in mice. *Circulation.* 2011;124(17):1819-29. doi: 10.1161/CIRCULATIONAHA.110.015974.
13. Aghababazadeh M, Dorraki N, Javan FA, Fattahi AS, Gharib M, Pasdar A.

Downregulation of Caspase 8 in a group of Iranian breast cancer patients - A pilot study. *J Egypt Natl Canc Inst.* 2017;29(4):191-5. doi: 10.1016/j.jnci.2017.10.001.
14. Fonin AV, Stepanenko OV, Sitdikova AK, Antifeeva IA, Kostyleva EI, Polyanichko AM, et al. Folding of poly-amino acids and intrinsically disordered proteins in overcrowded milieu induced by pH change. *Int J Biol Macromol.* 2019;125:244-55. doi: 10.1016/j.ijbiomac.2018.12.038.
15. Santos J, Iglesias V, Pintado C, Santos-Suárez J, Ventura S. DispHred: A server to predict pH-dependent order-disorder transitions in intrinsically disordered proteins. *Int J Mol Sci.* 2020;21(16):5814. doi: 10.3390/ijms21165814.
16. McIlwain DR, Berger T, Mak TW. Caspase functions in cell death and disease. *Cold Spring Harb Perspect Biol.* 2013;5(4):a008656. doi: 10.1101/cshperspect.a008656. Erratum in: *Cold Spring Harb Perspect Biol.* 2015;7(4). pii: a026716. doi: 10.1101/cshperspect.a026716.
17. Krzywinski M, Schein J, Birol I, Connors J, Gascoyne R, Horsman D, et al. Circos: an information aesthetic for comparative genomics. *Genome Res.* 2009;19(9):1639-45. doi: 10.1101/gr.092759.109.
18. Santos J, Iglesias V, Pintado C, Santos-Suárez J, Ventura S. DispHred: A server to predict pH-dependent order-disorder transitions in intrinsically disordered proteins. *Int J Mol Sci.* 2020;21(16):5814. doi: 10.3390/ijms21165814.
19. Zamora WJ, Campanera JM, Luque FJ. Development of a structure-based, pH-dependent lipophilicity scale of amino acids from continuum solvation calculations. *J Phys Chem Lett.* 2019;10(4):883-9. doi: 10.1021/acs.jpclett.9b00028.
20. Iglesias V, Pintado-Grima C, Santos J, Fornt M, Ventura S. Prediction of the effect of pH on the aggregation and conditional folding of intrinsically disordered proteins with SolupHred and DispHred. *Methods Mol Biol.* 2022;2449:197-211. doi: 10.1007/978-1-0716-2095-3_8.
21. Tian W, Chen C, Lei X, Zhao J, Liang J. CASTp 3.0: computed atlas of surface topography of proteins. *Nucleic Acids Res.* 2018;46(W1):W363-W367. doi: 10.1093/nar/gky473.
22. Rasoulpoor S, Asgharzadeh MR, Shabani S. A mimic of the tumor microenvironment on GPR30 gene expression in breast cancer. *Multidiscip Cancer Invest.* 2022;6(2):1-8.
23. Zhang Y, Peng Q, Zheng J, Yang Y, Zhang X, Ma A, et al. The function and mechanism of lactate and lactylation in tumor metabolism and microenvironment. *Genes Dis.* 2022;10(5):2029-37. doi: 10.1016/j.gendis.2022.10.006.
24. Lauritzen G, Jensen MB, Boedtkjer E, Dybboe R, Aalkjaer C, Nylandsted J, et al. NBCn1 and NHE1 expression and activity in DeltaNErbB2 receptor-expressing MCF-7 breast cancer cells: contributions to pHi regulation and chemotherapy resistance. *Exp Cell Res.* 2010;316(15):2538-53.
25. Toft NJ, Axelsen TV, Pedersen HL, Mele M, Burton M, Balling E, et al. Acid-base transporters and pH dynamics in human breast carcinomas predict proliferative activity, metastasis, and survival. *Elife.* 2021;10:e68447.
26. Lee S, Toft NJ, Axelsen TV, Espejo MS, Pedersen TM, Mele M, et al. Carbonic anhydrases reduce the acidity of the tumor microenvironment, promote immune infiltration, decelerate tumor growth, and improve survival in ErbB2/HER2-enriched breast cancer. *Breast Cancer Res.* 2023;25(1):46. doi: 10.1186/s13058-023-01644-1.
27. Wong P, Kleemann HW, Tannock IF. Cytostatic potential of novel agents that inhibit the regulation of intracellular pH. *Br J*

Cancer. 2002;87(2):238-45. doi: 10.1038/sj.bjc.6600424.
28. McDonald PC, Chafe SC, Supuran CT, Dedhar S. Cancer therapeutic targeting of hypoxia induced carbonic anhydrase IX: from bench to bedside. *Cancers (Basel).* 2022;14(14):3297. doi: 10.3390/cancers14143297.
29. Cardone RA, Casavola V, Reshkin SJ. The role of disturbed pH dynamics and the Na+/H+ exchanger in metastasis. *Nat Rev Cancer*. 2005;5(10):786-95.
30. Boedtkjer E, Moreira JM, Mele M, Vahl P, Wielenga VT, Christiansen PM, et al. Contribution of Na+,HCO3(-)-cotransport to cellular pH control in human breast cancer: a role for the breast cancer susceptibility locus NBCn1 (SLC4A7). *Int J Cancer.* 2013;132(6):1288-99. doi: 10.1002/ijc.27782.
31. Chen Y, Choong LY, Lin Q, Philp R, Wong CH, Ang BK, et al. Differential expression of novel tyrosine kinase substrates during breast cancer development. *Mol Cell Proteomics.* 2007;6(12):2072-87. doi: 10.1074/mcp.M700395-MCP200.
32. Hagemann T, Wilson J, Burke F, Kulbe H, Li NF, Plüddemann A, et al. Ovarian cancer cells polarize macrophages toward a tumor-associated phenotype. *J Immunol.* 2006;176(8):5023-32.
33. Mandal R, Raab M, Rödel F, Krämer A, Kostova I, Peña-Llopis S, et al. The non-apoptotic function of Caspase-8 in negatively regulating the CDK9-mediated Ser2 phosphorylation of RNA polymerase II in cervical cancer. *Cell Mol Life Sci.* 2022;79(12):597. doi: 10.1007/s00018-022-04598-3. Erratum in: *Cell Mol Life Sci.* 2023;80(3):64.
34. Hernandez L, Kim MK, Noonan AM, Sagher E, Kohlhammer H, Wright G, et al. A dual role for Caspase8 and NF-κB interactions in regulating apoptosis and necroptosis of ovarian cancer, with correlation to patient survival. *Cell Death Discov.* 2015;1:15053. doi: 10.1038/cddiscovery.2015.53.
35. Nowak M, Klink M. The role of tumor-associated macrophages in the progression and chemoresistance of ovarian cancer. *Cells.* 2020;9(5):1299. doi: 10.3390/cells9051299.
36. Maelfait J, Beyaert R. Non-apoptotic functions of caspase-8. *Biochem Pharmacol.* 2008;76(11):1365-73. doi: 10.1016/j.bcp.2008.07.034.
37. Afzaljavan F, Vahednia E, Barati Bagherabad M, Vakili F, Moezzi A, Hosseini A, et al. Genetic contribution of caspase-8 variants and haplotypes to breast cancer risk and prognosis: a case-control study in Iran. *BMC Med Genomics.* 2023;16(1):72. doi: 10.1186/s12920-023-01484-0.
38. Moelbert S, Emberly E, Tang C. Correlation between sequence hydrophobicity and surface-exposure pattern of database proteins. *Protein Sci.* 2004;13(3):752-62.
39. Rapaport DC. Configurational properties of polymers in a good solvent. *J Phys A Math Gen.* 1976;9(9):1521-37. doi:10.1088/0305-4470/9/9/013.

Table 1. The sequences of desired genes

Genes	Forward primer	Reverse primer
SLC4A7	5´-CCAGTCGGATTCCTCTTGTTCG-3´	5´-CAGACCTGTTCGCAAAGAGTGG-3´
Caspase-3	5´-GGAAGCGAATCAATGGACTCTG-3´	5´-GCATCGACATCTGTACCAGACC-3´
β-actin	5´-CACCATTGGCAATGAGCGGTTC-3	5´-AGGTCTTTGCGGATGTCCACGT-3´

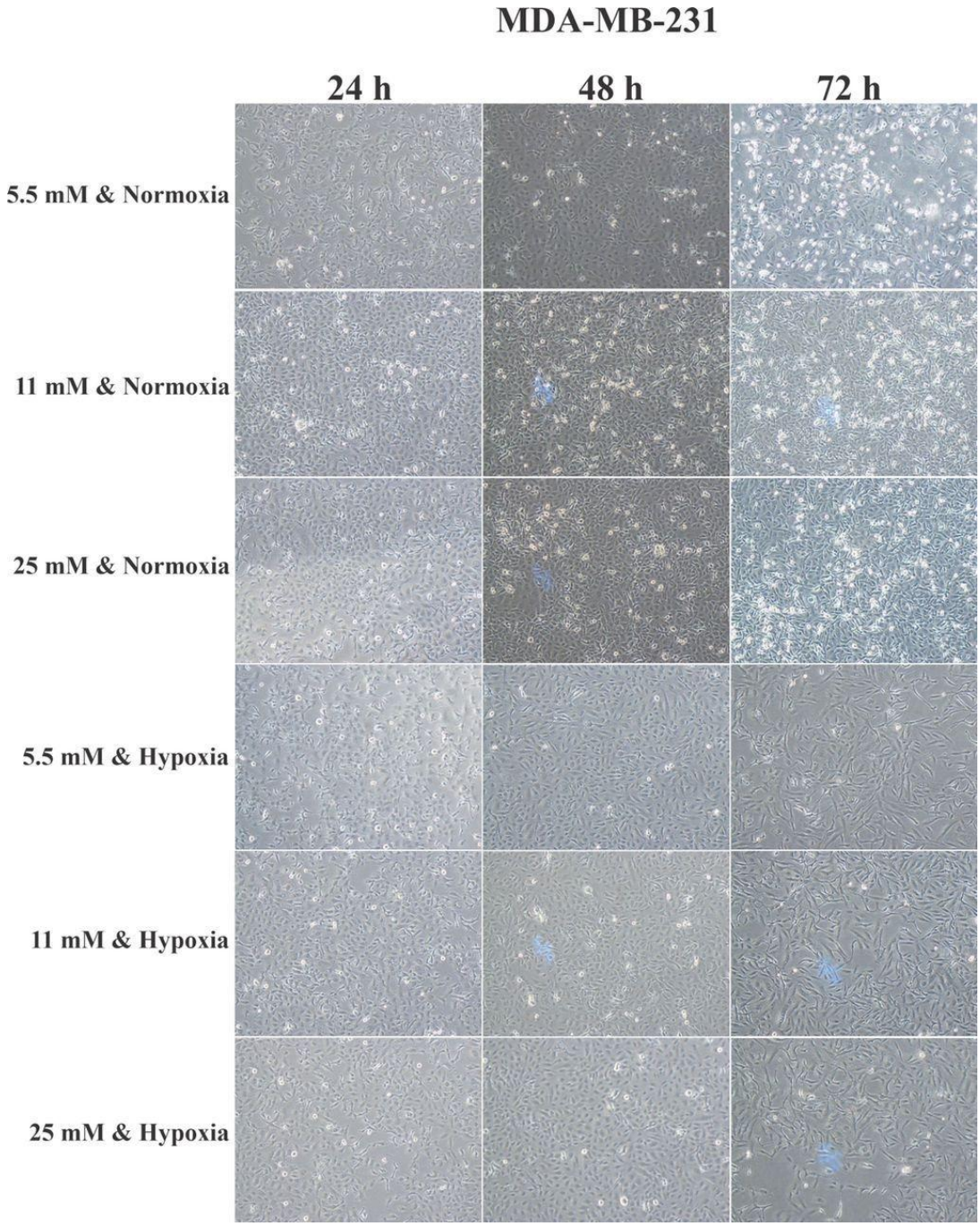

Figure 1. This figure shows the in vitro effects of glucose concentration and hypoxia on MDA-MB-231 cell morphology. The series of photomicrographs depict MDA-MB-231 cells after incubation periods of 24, 48, and 72 hours under varying glucose concentrations (5.5, 11, and 25 mM) and oxygen conditions (normoxia and hypoxia). These images provide a visual representation of the cellular morphological changes in response to the experimental conditions.[22]

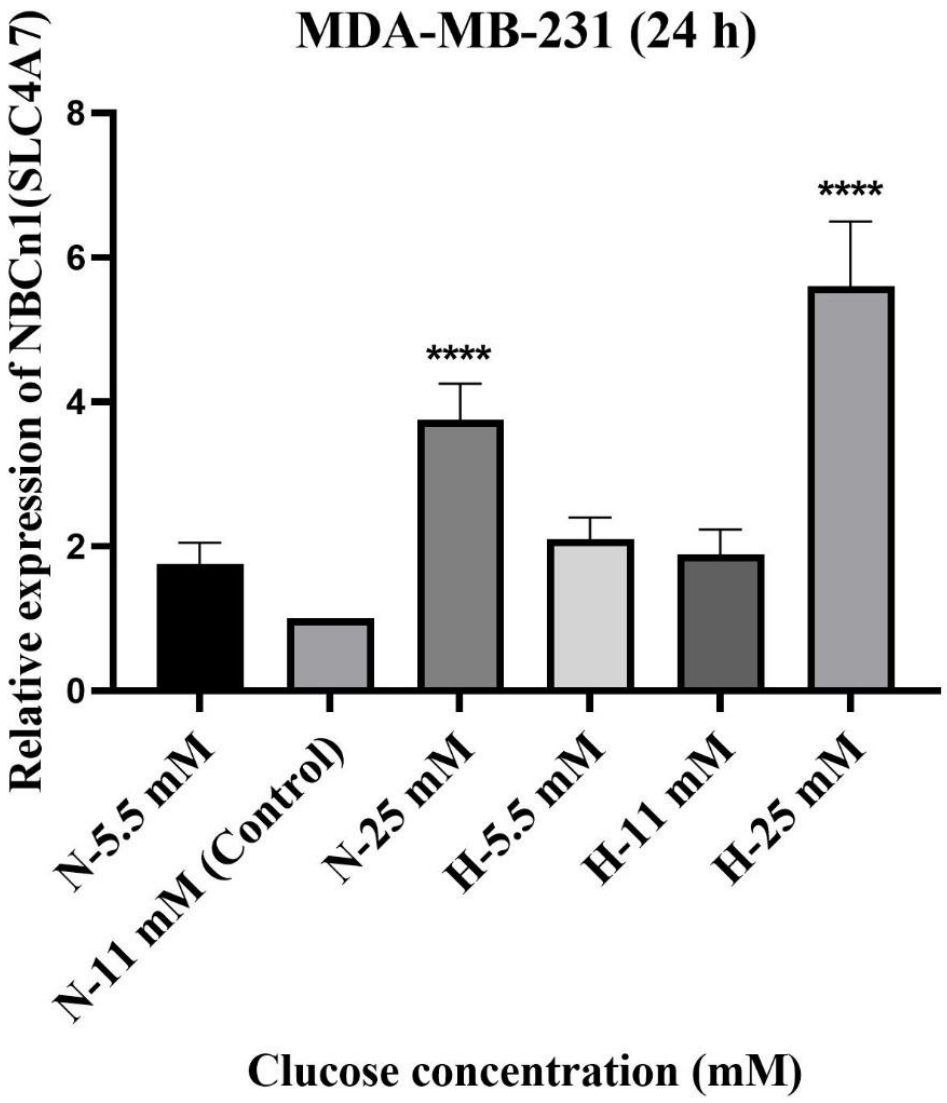

Figure 2. This figure presents the relative expression of the SLC4A7 (NBCn1) gene in MDA-MB-231 cell lines following a 24-hour incubation period. The data are expressed as means ± SD. One-way ANOVA was utilized for the statistical analysis of the results.
$^{*}P \leq 0.05$, $^{**}P \leq 0.01$, $^{***}P \leq 0.001$, and $^{****}P \leq 0.0001$

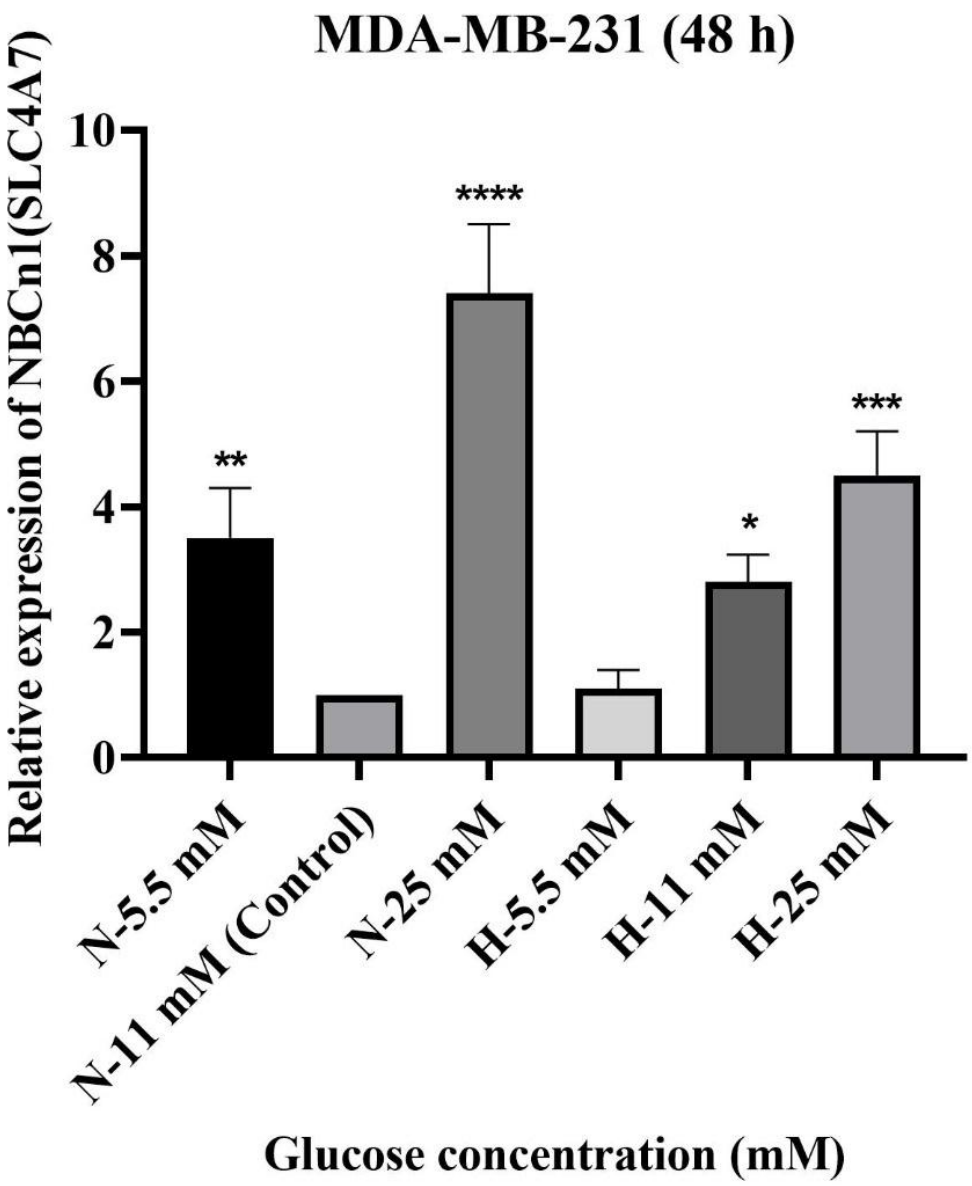

Figure 3. This figure illustrates the relative expression levels of the SLC4A7 (NBCn1) gene in MDA-MB-231 cell lines after a 48-hour incubation period. The data are represented as means ± SD. One-way ANOVA was employed to perform the statistical analysis of the data.
$^{*}P \leq 0.05$, $^{**}P \leq 0.01$, $^{***}P \leq 0.001$, and $^{****}P \leq 0.0001$

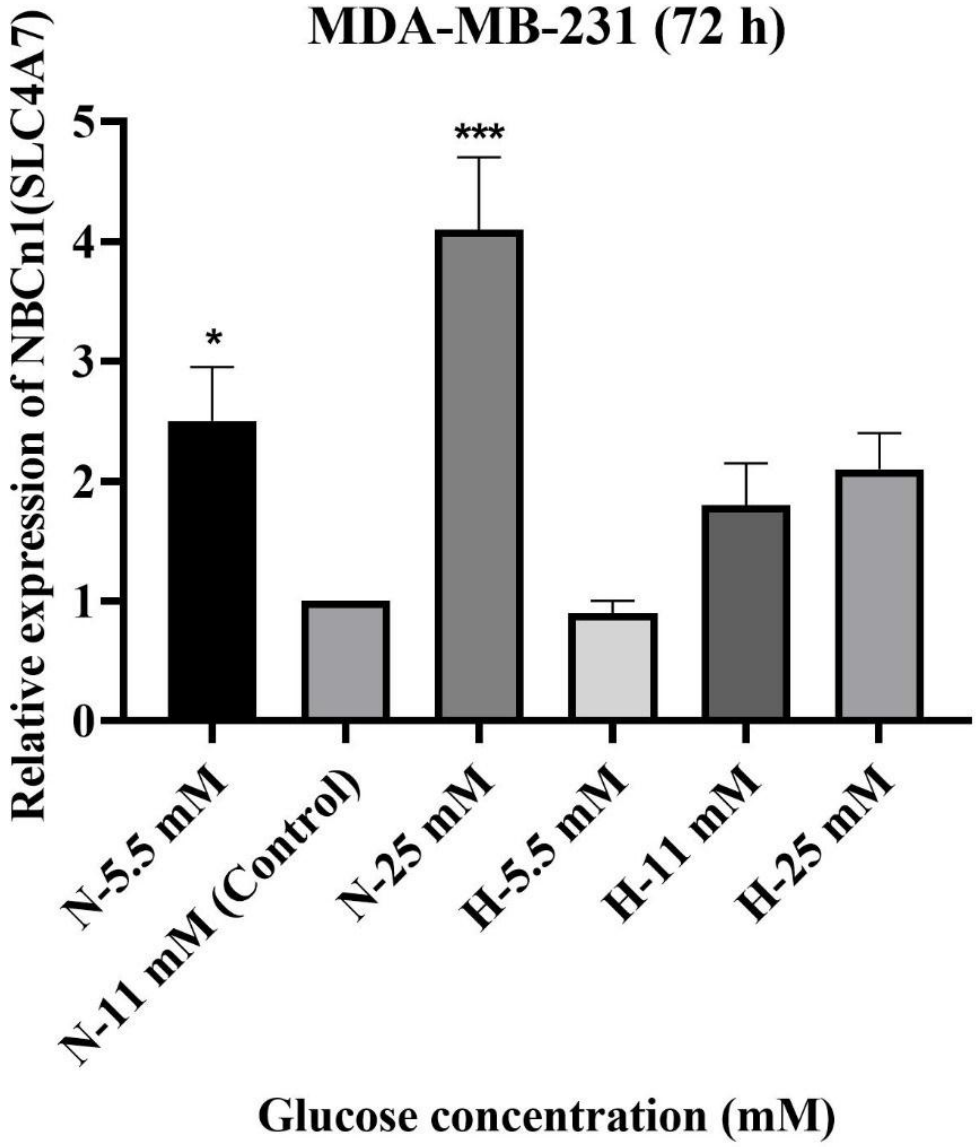

Figure 4. This figure displays the relative expression of the SLC4A7 (NBCn1) gene in MDA-MB-231 cell lines after a 72-hour incubation period. One-way ANOVA was utilized for the statistical analysis.

$^{*}P \leq 0.05$, $^{**}P \leq 0.01$, $^{***}P \leq 0.001$, and $^{****}P \leq 0.0001$

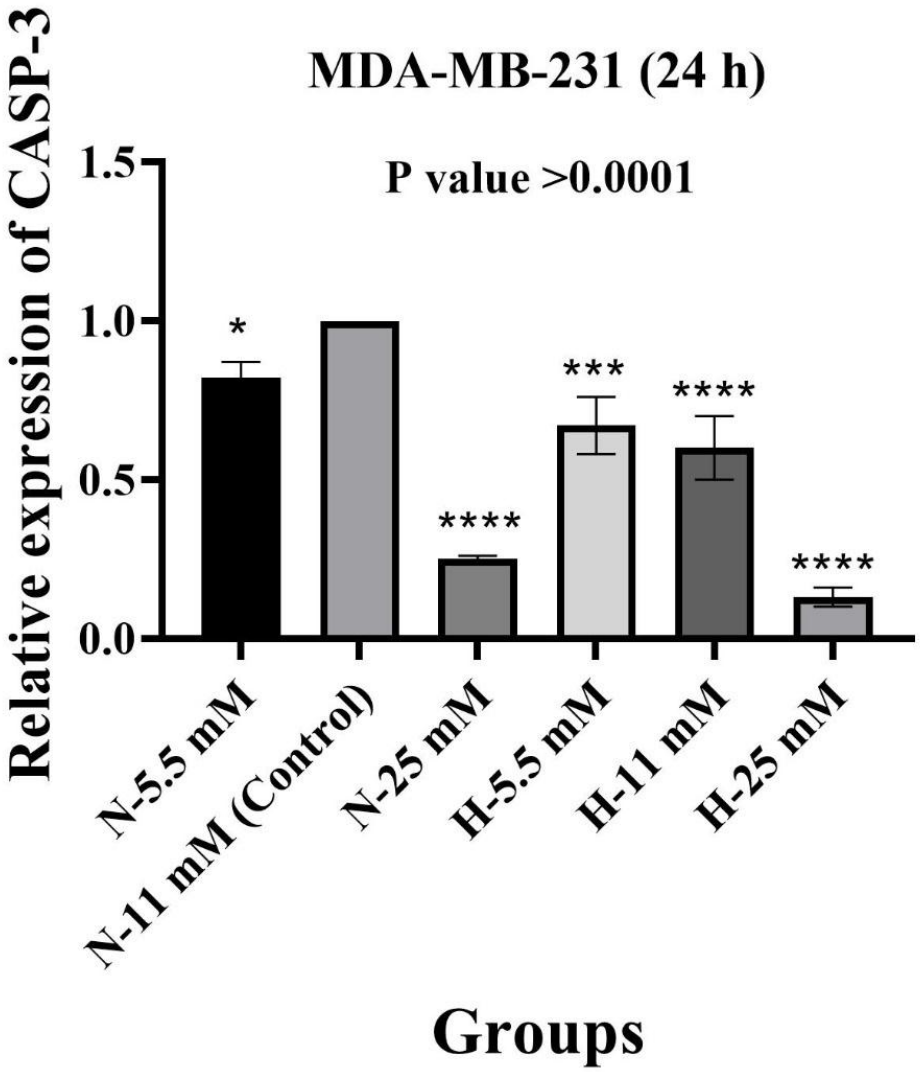

Figure 5. This figure depicts the relative expression of the caspase-3 gene in MDA-MB-231 cell lines after a 24-hour incubation period. The data are presented as mean ± SD. One-way ANOVA was employed for the statistical analysis.

$^{*}P \leq 0.05$, $^{**}P \leq 0.01$, $^{***}P \leq 0.001$, and $^{****}P \leq 0.0001$

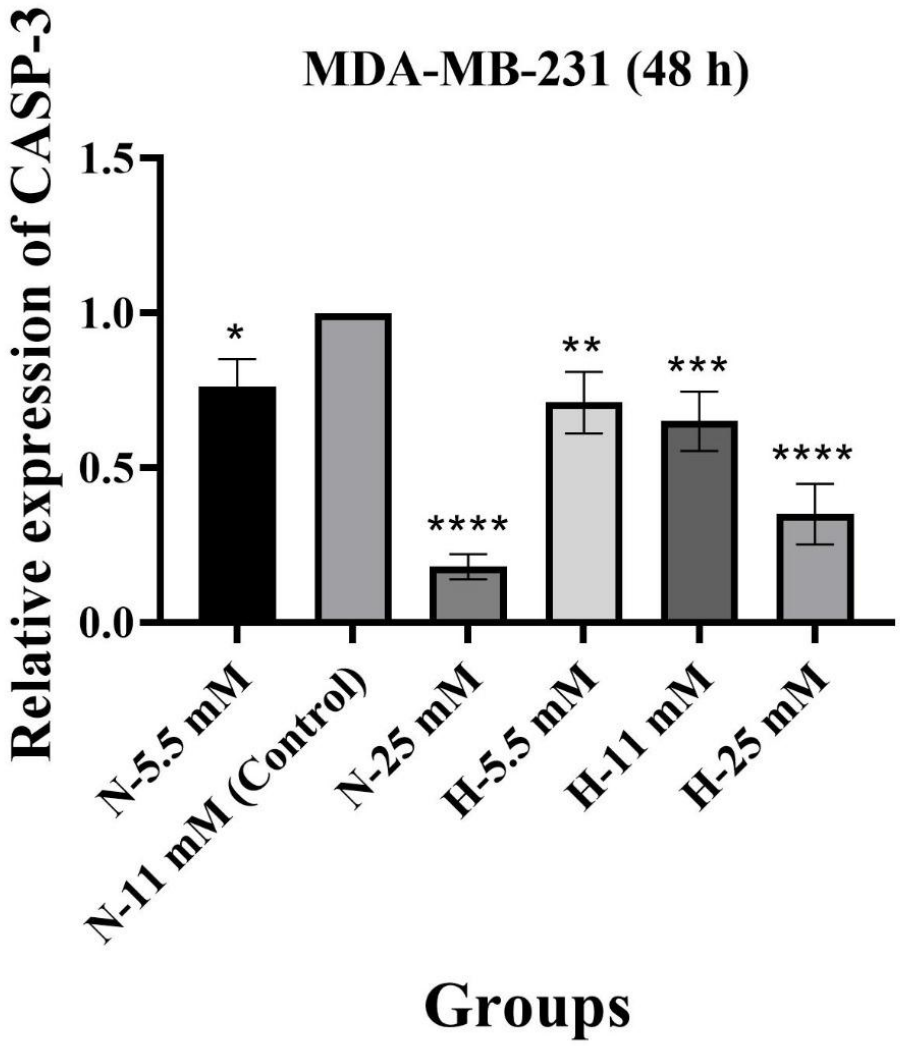

Figure 6. This figure illustrates the relative expression levels of the caspase-3 gene in MDA-MB-231 cell lines following a 48-hour incubation period. The data are presented as mean ± SD. One-way ANOVA was employed for the statistical analysis of the data.
$^{*}P \leq 0.05$, $^{**}P \leq 0.01$, $^{***}P \leq 0.001$, and $^{****}P \leq 0.0001$

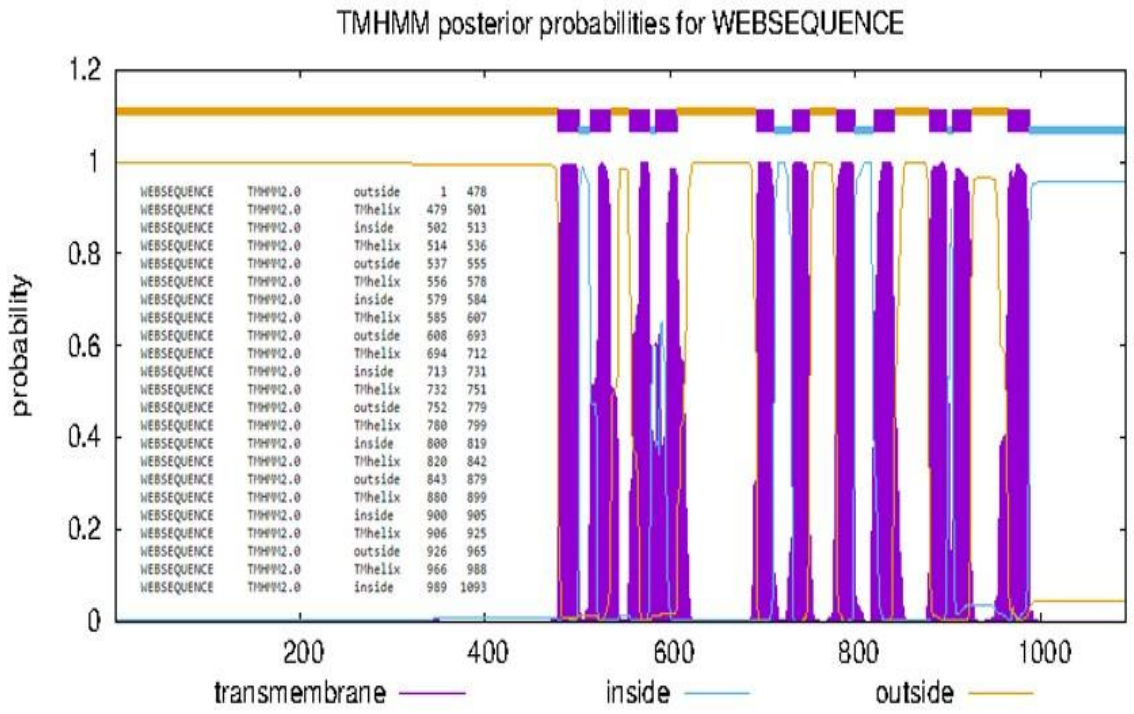

Figure 7. The analysis from the TMHMM server indicates that NBCn1 functions as a transmembrane protein. This protein spans a length of 1093 amino acids and is characterized by the presence of 11 TMHs. These structural details are graphically represented and accompanied by the sequence information in the corresponding figure.

TMHMM: Transmembrane helices; Hidden Markov model; TMHs: Transmembran helixes

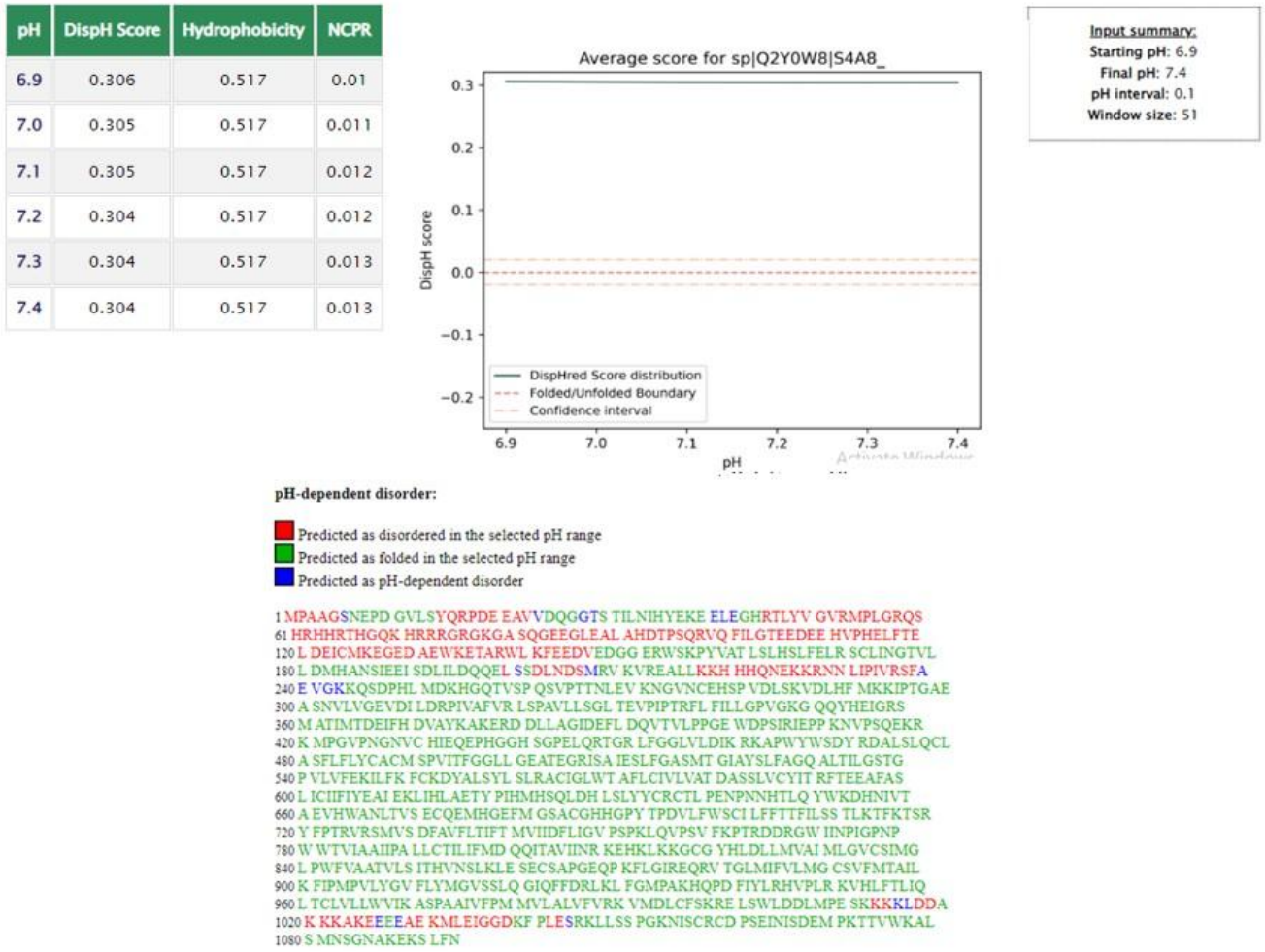

Figure 8. DispHred web server results. DispHred is a protein disorder predictor over pH for proteins. This server tracks disorder in pHs. The table shows the DispHred, hydrophobicity, and NCPR in a given pH. A figure represents the DispH average score for each pH, and the score above the red dashed line shows the predicted order. Folded, unfolded, and conditionally unfolded compartments are exhibited in sequence in green, red, and blue, respectively. Positive and negative amounts of DispH are various colors. Proteins with NCPR below a threshold value of 0.25 are equal with compact globular and stable conformations, whereas sequences above this threshold show well-solvated and disordered enlarged coils (Figure 8).

NCPR: Net charge per residue

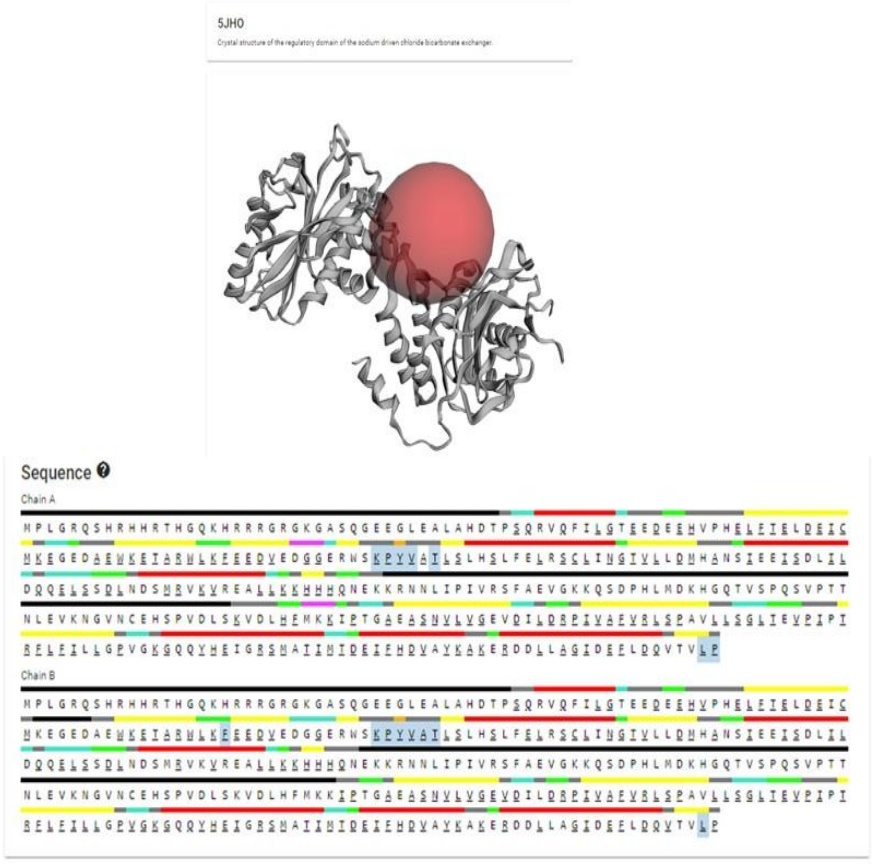

Figure 9. The result from the CASTp 3.0 server. The result from the CASTp 3.0 server showed that the binding pocket is located on both subunits. Lys102, Pro103, Tyr104, Val105, Thr107, Leu343, and Pro344 from A chain make binding pockets. Phe89, Lys102, Pro103, Tyr104, Val105, Ala106, Thr107, and Leu343 from the B chain are involved in making binding pockets.
CASTp 3.0: Computed atlas of surface topography of proteins

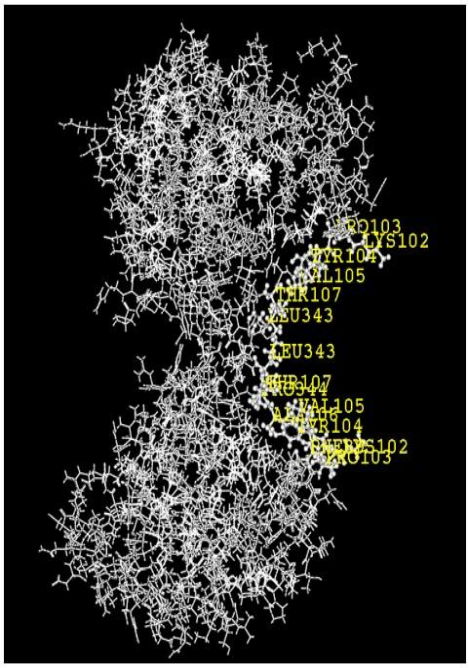

Figure 10. The amino acids are involved in making the binding pocket. A_{Lys102}, A_{Pro103}, A_{Tyr104}, $AVal_{105}$, A_{Thr107}, A_{Leu343} A_{Pro344} B_{Phe89}, B_{Lys102}, B_{Pro103}, B_{Tyr104}, B_{Val105}, B_{Ala106}, BT_{hr107} and B_{Leu343} are involved in making binding pocket.